Magnetic resonance elastography to study the effect of amyloid plaque accumulation in a mouse model

Miklos Palotai, Katharina Schregel, Navid Nazari, Julie Merchant, Walter Taylor, Charles Guttmann, Ralph Sinkus, Tracy Young-Pearse, Samuel Patz

Received: 18 January 2022 | Revised: 14 March 2022 | Accepted: 17 March 2022

DOI: 10.1111/jon.12996

JOURNAL OF NEUROIMAGING
THE OFFICIAL JOURNAL OF THE AMERICAN SOCIETY OF NEUROIMAGING
WILEY

EXPERIMENTAL LABORATORY RESEARCH

Magnetic resonance elastography to study the effect of amyloid plaque accumulation in a mouse model

Miklos Palotai[1,2] | Katharina Schregel[1,2,3,4] | Navid Nazari[1,5] | Julie P. Merchant[6] | Walter M. Taylor[6] | Charles R. G. Guttmann[1,2] | Ralph Sinkus[7,8] | Tracy L. Young-Pearse[2,6] | Samuel Patz[1,2]

[1]Department of Radiology, Brigham and Women's Hospital, Boston, Massachusetts, USA

[2]Harvard Medical School, Boston, Massachusetts, USA

[3]Institute of Neuroradiology, University Medical Center Göttingen, Göttingen, Germany

[4]Department of Neuroradiology, Heidelberg University Hospital, Heidelberg, Germany

[5]Department of Biomedical Engineering, Boston University, Boston, Massachusetts, USA

[6]Ann Romney Center for Neurologic Diseases, Brigham and Women's Hospital, Boston, Massachusetts, USA

[7]School of Biomedical Imaging and Imaging Sciences, King's College London, London, UK

[8]INSERM U1148, Laboratory for Vascular Translational Science, University Paris Diderot, University Paris 13, Paris, France

Correspondence
Miklos Palotai, Department of Radiology, Brigham and Women's Hospital, Harvard Medical School, 1249 Boylston Street, Boston, MA 02215, USA.
Email: palotai@bwh.harvard.edu

Funding information
This work was supported by the National Institutes of Health (grant number NIH R21 EB020757), the European Commission Horizon 2020 (proposal 668039) and from Boston University College of Engineering and the Brigham and Women's Hospital Department of Radiology. K.S. received funding from the German Research Foundation (DFG, SCHR 1542/1-1).

Abstract

Background and Purpose: Biomechanical changes in the brain have not been fully elucidated in Alzheimer's disease (AD). We aimed to investigate the effect of β-amyloid accumulation on mouse brain viscoelasticity.

Methods: Magnetic resonance elastography was used to calculate magnitude of the viscoelastic modulus ($|G^*|$), elasticity (G_d), and viscosity (G_l) in the whole brain parenchyma (WB) and bilateral hippocampi of 9 transgenic J20 (AD) mice (5 males/4 females) and 10 wild-type (WT) C57BL/6 mice (5 males/5 females) at 11 and 14 months of age.

Results: Cross-sectional analyses showed no significant difference between AD and WT mice at either timepoints. No sex-specific differences were observed at 11 months of age, but AD females showed significantly higher hippocampal $|G^*|$ and G_l and WB $|G^*|$, G_d, and G_l compared to both AD and WT males at 14 months of age. Similar trending differences were found between female AD and female WT animals but did not reach significance. Longitudinal analyses showed significant increases in hippocampal $|G^*|$, G_d, and G_l, and significant decreases in WB $|G^*|$, G_d, and G_l between 11 and 14 months in both AD and WT mice. Each subgroup showed significant increases in all hippocampal and significant decreases in all WB measures, with the exception of AD females, which showed no significant changes in WB $|G^*|$, G_d, or G_l.

Conclusion: Aging had region-specific effects on cerebral viscoelasticity, namely, WB softening and hippocampal stiffening. Amyloid plaque deposition may have sex-specific effects, which require further scrutiny.

KEYWORDS
Alzheimer's disease, brain parenchyma, hippocampus, J20 mice, magnetic resonance elastography, MRE, sex

INTRODUCTION

Alzheimer's disease (AD) is a progressive neurodegenerative disease representing the most common cause of dementia worldwide. Clinically, AD is characterized by the development of multiple cognitive deficits, including decline in memory and learning, aphasia, and disturbance in executive functions. Histopathological hallmarks of AD include extracellular amyloid β (Aβ) deposits and intracellular neurofibrillary tangles, which lead to hyperactivation of astrocytes and microglia, neuronal dysfunction, loss of synaptic connections, and ultimately cell death. These changes appear first in the hippocampal formation and entorhinal cortex and eventually spread to the entire brain.[1–4]

Magnetic resonance elastography (MRE) is a noninvasive in vivo imaging technique that enables the quantitative investigation of biomechanical tissue properties, such as tissue elasticity (G_d) and viscosity (G_l).[5] MRE is performed by inducing tiny mechanical shear waves into a tissue of interest, typically by placing a nonmagnetic vibrating transducer on an external surface near the tissue of interest. Motion-encoding magnetic field gradients are applied synchronously with the mechanical vibration to measure the time-dependent displacement of the shear waves. The displacement is then used as input to an inversion of the Navier wave equation to estimate biomechanical properties, which are then displayed as maps, also called elastograms, of elasticity, viscosity, or the magnitude of the viscoelastic modulus (|G*|).[6–8]

Previous studies have shown that AD is associated with softening of the human brain.[9–12] These findings suggest that the stiffness of brain tissue may serve as a noninvasive biomarker for neurodegenerative changes.[13] However, the underlying biomechanical mechanisms have not been fully elucidated, nor is it clear if this stiffness precedes the overt cell death that occurs as the disease progresses.

Three previous studies investigated the effects of Aβ plaque accumulation on biomechanical tissue properties of the brain using transgenic mouse model of AD at 2, 4, 6, and 20 months of age.[14–16] These studies associated AD with softening of the whole brain (WB) parenchyma[15,16] and the hippocampus.[14,16] Of note, 6 months of age in mice corresponds to ~30 years of age in humans, while the age of 20 months in mice is equivalent to the age of ~60 years in humans.[17]

The aim of our study was to investigate the effects of Aβ plaque accumulation on whole brain (WB) and hippocampal viscoelasticity in 11 and 14 months old transgenic J20 mice, the age of which corresponds to middle age (40-50 years) in humans.[17] We hypothesized that Aβ plaque accumulation is associated with brain softening in 11 and 14 months J20 mice compared to wild-type (WT) mice. We also investigated sex-specific differences in WB and hippocampal stiffness as well as the correlation of MRE parameters with WB Aβ load.

METHODS

Animals and study design

All experiments were performed in accordance with the Brigham and Women's Hospital Institutional Animal Care and Use Committee and ARRIVE guidelines.[18] Nine amyloidogenic transgenic J20 (AD) mice (5 males/4 females)[19] and 10 WT C57BL/6 mice (5 males/5 females) were used (Jackson laboratory, USA). In J20 mice, extracellular Aβ plaque deposition starts in the hippocampus at 1 month of age, and widespread plaque deposition develops by 8-10 months, with region-specific neuronal loss, synaptic loss, and gliosis, but without neurofibrillary tangle accumulation.[19–21] The J20 model expresses a minigene encoding human amyloid precursor protein (APP) carrying both the Swedish (KM670N/671NL) and Indiana (V717F) mutations, driven by the human platelet-derived growth factor beta polypeptide (PDGFB) promoter.

AD and WT mice underwent brain MRI and MRE at the average ages of 3, 8, 11, and 14 months. Note that scans were acquired ± a few weeks of the nominal timepoint. After the 8- and 14-month brain imaging sessions, a subset of mouse brains were harvested for biochemical and immunohistochemical analyses. Figure 1 shows the experimental outline. In AD mice, amyloid deposition is progressive with widespread plaques by 8-10 months.[20,21] In the current study, we analyzed only the 11- and 14-month MRI and MRE data. Since differences were observed only at the 14-month, but not at the 11-month timepoint, we did not revisit the 3- and 8-month data to perform further analyses.

MRI and MRE

MRI and MRE were performed on a 7T horizontal bore Bruker small animal scanner (Ettlingen, Germany; gradient strength 660 mT/m) using an 8.6-cm body coil for transmission and a 2-cm surface coil for reception. Imaging was performed under anesthesia, which was induced by 2.5% isoflurane in 100% O_2 and maintained by 1%-1.5% isoflurane in 100% O_2 delivered via a nose cone. Respiration rate was constantly monitored (SA Instruments, Stony Brook, NY, USA). The animals were placed prone on a custom-built bed, and an external transducer vibrating at 1 kHz transmitted mechanical vibrations to the bed as described in our previous work.[22]

The following imaging sequences were performed: (1) coronal T2-weighted RARE (TR/TE = 5000/56 ms; FOV = 19.2 mm; matrix = 192 × 192; slice thickness = 0.3 mm; number of averages = 6; number of slices = 9; acquisition time = 12 minutes) and (2) a customized multi-slice, single spin echo MRE sequence [23] (TR/TE = 900/29 ms; FOV = 19.2 mm; matrix = 64 × 64; isotropic resolution 0.3 mm; number of averages = 1; number of wave phases = 8; number of slices = 9; acquisition time = 23 minutes). RARE and MRE covered identical volumes and were positioned in the hippocampus-bearing region. Anatomical borders of the hippocampi were defined using a stereotaxic mouse brain atlas.[24]

MRE data were reconstructed using dedicated in-house software (ROOT environment, CERN, Meyrin, Switzerland) according to published algorithms.[6,25] The phase data are unwrapped for each slice and then aligned between slices. Since eight wave-phases were acquired, an 8-point Fourier transform is calculated and the first harmonic amplitude is used to represent the displacement amplitude at our vibration frequency of 1 kHz. The curl of the displacement data is taken to get rid of any compression waves and then spatial derivates are

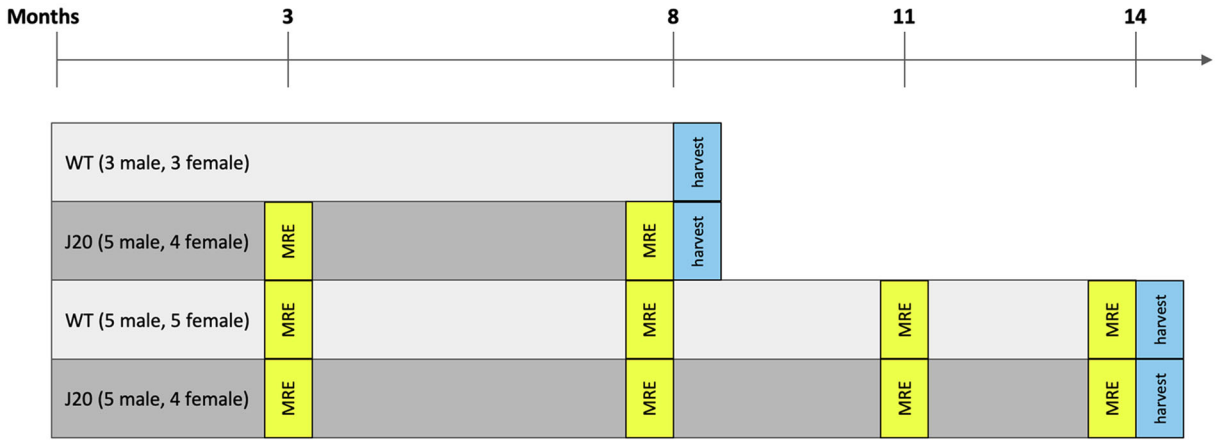

FIGURE 1 Experimental outline. Magnetic Resonance Elastography was performed at 3, 8, 11, and 14 months of age on transgenic J20 as well as wild-type mice. Mouse brains were harvested for biochemical and immunohistochemical analyses at 8 and 14 months of age. WT, wild-type

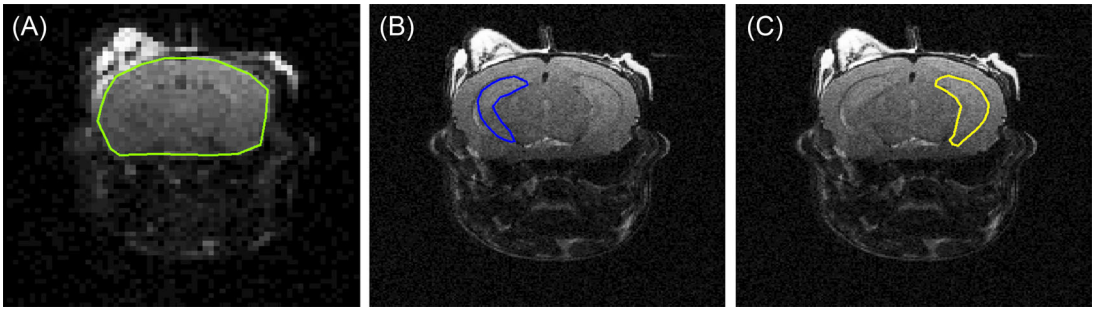

FIGURE 2 Manual segmentation maps of regions of interest overlaid on brain Magnetic Resonance images. Whole brain (A) was segmented on the Magnetic Resonance Elastography magnitude image, whereas right (B) and left (C) hippocampi were segmented on T2-weighted MRI images

calculated to be used for inversion of Navier's equation. (Note that because second-order derivatives are used in the elastogram reconstruction, of the original acquired 9 slices, one only obtains results for slices 3-7). T2-weighted RARE images were displayed in the same software and used as anatomical references. The WB parenchyma (including the hippocampi and ventricles) was manually segmented on MRE magnitude images (Figure 2). Left and right hippocampi were manually segmented slice-by-slice on T2-weighted RARE images, since anatomical boundaries of the hippocampus cannot be determined on our MRE images. The hippocampal segmentations were then overlaid onto the elastograms. The following MRE parameters were investigated: elasticity (storage modulus, G_d), viscosity (loss modulus, G_l), and viscoelastic modulus ($|G^*| = \sqrt{G_d^2 + G_l^2}$). These MRE parameters were calculated for each region-of-interest (ROI). The right and left hippocampal MRE parameters were averaged.

Amyloid β sequential extraction and quantification

Animals were euthanized by CO_2 inhalation overdose, after which brains were quickly dissected and divided sagittally. The left cerebral hemisphere was immediately fixed in 4% paraformaldehyde and stored at 4°C for sectioning and immunohistochemistry. The right hemisphere was immediately frozen on dry ice and stored at −80°C for biochemical analysis.

To extract monomeric/oligomeric forms of Aβ, frozen right hemispheres were homogenized using a mechanical Potter-Elvehjem homogenizer (Wheaton) with 20 strokes in ice-cold BrainPhys™ Neuronal Medium (STEMCELL Technologies) at 2.5:1 (volume:brain wet weight). Homogenates were centrifuged in a TLA 120.2 rotor (Beckman Coulter) at 175,000 × *g* and 4°C for 30 minutes. The supernatants (denoted "BrainPhys extracts") were removed and transferred to clean tubes. All samples (supernatants and pellets) were then stored at −80°C until further use.

To extract lipid-associated Aβ, each pellet remaining from the BrainPhys extraction was re-homogenized with 20 strokes by hand in ice-cold 1% Triton X-100 in TBS (TBS-TX) at 4:1 (volume:starting brain wet weight). Homogenates were centrifuged at 175,000 × *g* and 4°C for 30 minutes, the supernatants ("TBS-TX extracts") were transferred to clean tubes, and all samples stored at −80°C.

Finally, to extract aggregated Aβ, each pellet remaining from the TBS-TX extraction was re-homogenized with 20 strokes by hand in 5.0 M guanidine HCl in 50 mM Tris-HCl, pH 8.0 (GuHCl) at 8:1 (volume:starting brain wet weight). Samples were incubated on a

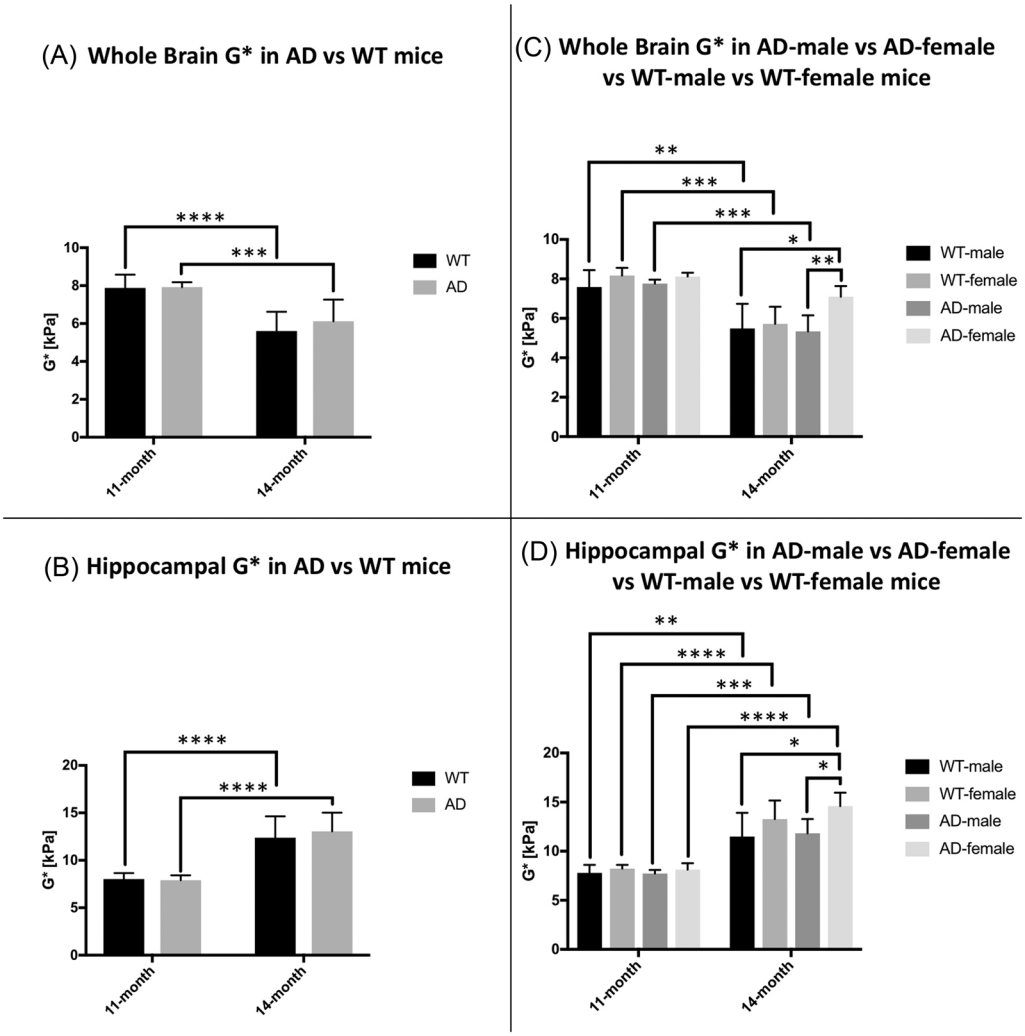

FIGURE 3 Cross-sectional and longitudinal comparisons of viscoelasticity (|G*|) in transgenic J20 versus wild-type mice at 11 and 14 months of age in the whole brain (A) and in the hippocampus (B). Cross-sectional and longitudinal comparisons of |G*| in the four subgroups according to genotype and sex at 11 and 14 months of age in the whole brain (C) and in the hippocampus (D). Asterisks indicate the level of significance as follows: $^{*}p < .05$, $^{**}p < .01$, $^{***}p < .001$, $^{****}p < .0001$. AD, transgenic J20; WT, wild-type

rocker for ~14 h at room temperature. The resulting solutions ("GuHCl extracts") were stored at −80°C.

Aβ levels in brain extracts were analyzed using the V-PLEX Aβ Peptide Panel 1 (6E10) Kit (Meso Scale Diagnostics). The levels of the monomeric/oligomeric, lipid-associated, and aggregated Aβ40 and Aβ42 were summed to calculate the total Aβ40 and Aβ42 burden, respectively.

Recent studies suggested that plasma[26] and cerebrospinal fluid[27] AB42/AB40 ratio may serve as biomarkers for detection of AD pathology. Therefore, we calculated AB42/AB40 ratio as well.

The two major neuropathological features for the diagnosis of AD (ie, extracellular plaque formation and neurofibrillary tangles) are mainly confined in the hippocampus and the cerebral cortex.[28] Our qualitative immunohistochemical analysis (please see details of the analysis under "Immunohistochemistry of brain sections") confirmed that amyloid plaques are indeed accumulated in the hippocampus and cerebral cortex of our J20 mice. These findings may support that whole brain amyloid level measures can serve a sufficient surrogate for inferring the hippocampal amyloid levels.

Immunohistochemistry of brain sections

The aim of this qualitative analysis was to assess whether amyloid plaques were deposited in the hippocampus and cortex of two transgenic J20 mice with the highest and the lowest aggregated amyloid β levels. Left hemispheres fixed in 4% paraformaldehyde were washed in phosphate-buffered saline (PBS), embedded in 2% agarose/PBS, and vibratome sectioned into 150 μm coronal sections. Sections were pretreated to quench endogenous peroxidases (10% H2O2; 0.1% PBS-Tween) for 30 minutes, followed by three PBS washes. Sections were then incubated in blocking buffer (2% goat serum; 0.1% Triton X-100 in PBS) for 1 hour, then incubated in primary antibody 3D6 (a monoclonal antibody that recognizes the extreme N-termini of Aβ) diluted

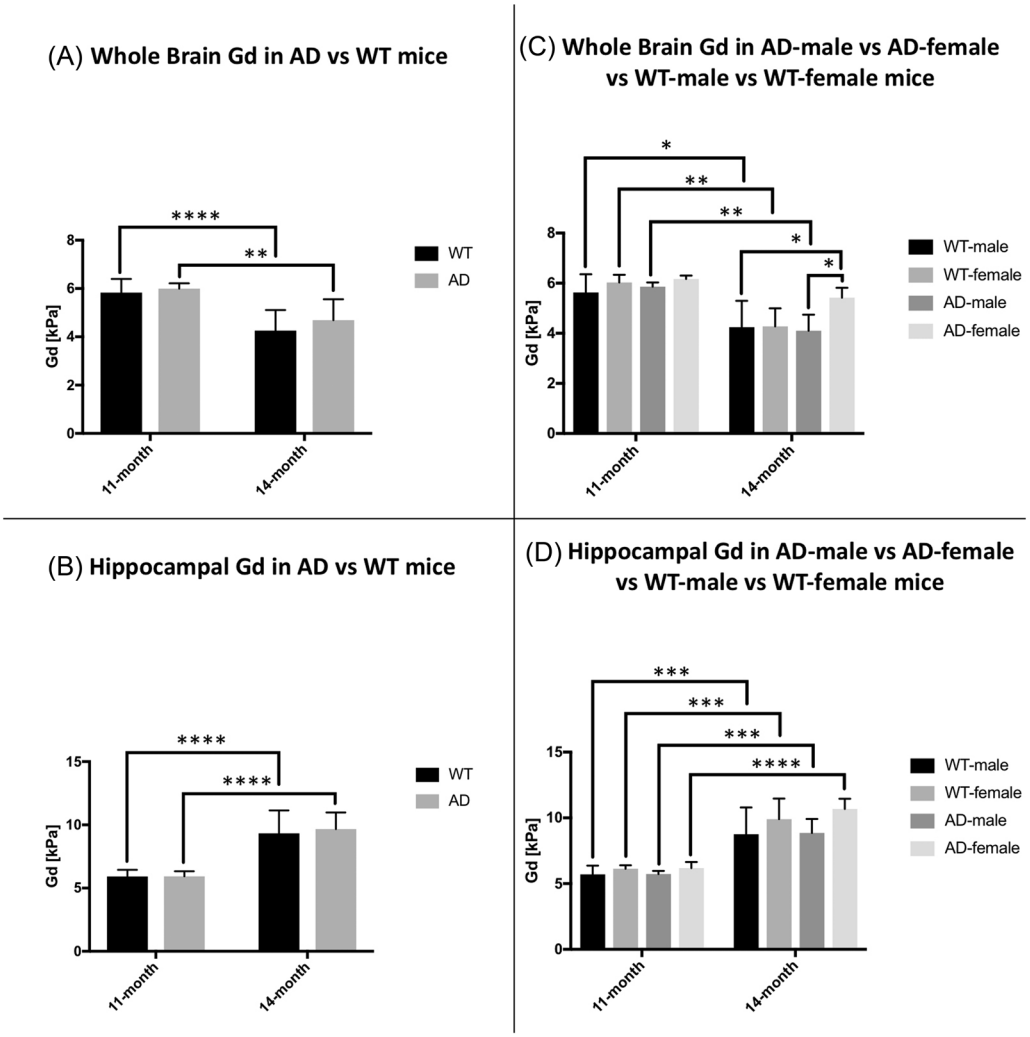

FIGURE 4 Cross-sectional and longitudinal comparisons of elasticity (Gd) in transgenic J20 versus wild-type mice at 11 and 14 months of age in the whole brain (A) and in the hippocampus (B). Cross-sectional and longitudinal comparisons of Gd in the four subgroups according to genotype and sex at 11 and 14 months of age in the whole brain (C) and in the hippocampus (D). Asterisks indicate the level of significance as follows: $^{*}p < .05$, $^{**}p < .01$, $^{***}p < .001$, $^{****}p < .0001$. AD, transgenic J20; WT, wild-type

in the same goat serum blocking buffer overnight at 4°C, followed by two PBS washes. Next, sections were incubated in a biotinylated IgG secondary antibody (1:100; Vector Laboratories) for 1 hour, followed by two PBS washes, then incubated in an avidin-biotin complex-based peroxidase solution (VECTASTAIN Elite ABC Kit, Vector Laboratories) for 1 hour, followed by two PBS washes. Finally, immunoreactivity was visualized using diaminobenzidine as the chromogen (DAB Substrate Kit, Vector Laboratories) for 2.5 minutes, followed by three washes in ddH_2O. Sections were mounted on glass slides using Fluoromount (Sigma) and images were acquired using a Zeiss Axioskop 2 plus with AxioCam HRc.

Statistical analysis

A two-way repeated-measures ANOVA with Sidak's post hoc test for multiple comparisons was used to perform (1) a cross-sectional comparison of the MRE parameters at each of the two timepoints in AD versus WT mice, as well as (2) a longitudinal investigation of the MRE parameters between the two timepoints in AD and WT mice separately. To investigate sex-specific differences, we repeated the abovementioned analyses in the following four subgroups: AD males, AD females, WT males, and WT females. To compare the magnitude of changes between 11 and 14 months of age (1) in AD versus WT mice as well as (2) in the abovementioned four subgroups, we used two-sample *t*-test and one-way ANOVA with Sidak's post hoc test, respectively. Total Aβ40 and Aβ42 levels as well as the Aβ42/Aβ40 ratio were compared between AD males and AD females at 8 and 14 months of age using two-sample *t*-tests. Pearson correlation was performed to investigate the association of WB MRE parameters with total Aβ40 and Aβ42 levels in AD mice at 14 months of age. Results of the analyses on the monomeric/oligomeric, lipid-associated, and aggregated Aβ40 and Aβ42 levels were overall similar to the results of the analyses on the total Aβ40 and Aβ42 levels. Therefore, we reported the

latter for easier interpretability. Two-way repeated-measures ANOVA was performed using GraphPad Prism 7 (GraphPad Software, La Jolla, CA, USA). Two-sample *t*-test, one-way ANOVA, and Pearson correlation were performed using Stata 13 (StataCorp, College Station, Texas, USA). The threshold for statistical significance was set to $p < .05$.

RESULTS

Cross-sectional analyses showed no difference in any MRE parameters of interest between AD and WT mice at either the 11- or 14-month timepoints. In addition, at the 11-month timepoint, there were no sex-specific differences between AD and WT mice. At the 14-month timepoint, however, there were differences between sexes. AD females showed significantly higher hippocampal |G*| ($p = .008$ vs. AD males) and G_l ($p = .002$ vs. AD males; $p = .003$ vs. WT males), as well as significantly higher WB |G*| ($p = .009$ vs. AD male; $p = .018$ vs. WT male), G_d ($p = .018$ vs. AD males; $p = .043$ vs. WT males), and G_l ($p = .005$ vs. AD males; $p = .006$ vs. WT males) compared to both AD and WT males, while differences with WT females were not statistically significant, but trended in the same direction ($p = .058$ for WB |G*|, $p = .052$ for G_d, $p = .077$ for G_l) (Figures 3-5; Table 1).

Longitudinal analyses showed significant increases in hippocampal |G*| ($p < .0001$ in both AD and WT), G_d ($p < .0001$ in both AD and WT mice), and G_l ($p < .0001$ in both AD and WT mice), as well as significant decreases in WB |G*| ($p = .0002$ in AD mice; $p < .0001$ in WT mice), G_d ($p = .001$ in AD mice; $p < .0001$ in WT mice), and G_l ($p = .0002$ in AD mice; $p < .0001$ in WT mice) between 11 and 14 months of age in both AD and WT mice. Each subgroup showed significant increases in hippocampal |G*| ($p < .0001$ in AD females; $p = .0005$ in AD males; $p < .0001$ in WT females; $p = .001$ in WT males), G_d ($p < .0001$ in AD females; $p = .0007$ in AD males; $p = .0001$ in WT females; $p = .0009$ in WT males), and G_l ($p < .0001$ in AD females; $p = .012$ in AD males; $p = .0006$ in WT females; $p = .002$ in WT males), as well as significant decreases in WB |G*| ($p = .0004$ in AD males; $p = .0003$ in WT females; $p = .001$ in WT males), G_d ($p = .002$ in AD males; $p = .002$ in WT females; $p = .012$ in WT males), and G_l ($p = .0001$ in AD males; $p = .0003$ in WT females; $p = .0001$ in WT males), with the exception of AD females, which showed no significant changes in WB |G*|, G_d, or G_l (Figures 3–6; Table 1).

The WB G_d and G_l were both higher in 3 out of 4 (75%) AD females compared to AD and WT males and WT females at the 14-month timepoint, but there was no clear distinction between these groups at the 11-month timepoint (Figure 7).

The magnitude of change in WB MRE parameters between 11 and 14 months of age did not show considerable difference in AD versus WT mice. In the four-subgroup comparison, hippocampal G_l was the only MRE parameter that showed a significant increase between 11 and 14 months of age in AD females versus WT males ($p = .045$), but not compared to WT females ($p = .691$) or AD males (0.152). The other hippocampal and WB MRE parameters did not show considerable differences between the four subgroups (ie, AD females, AD males, WT females, WT males). Figure 8 shows elastograms of 2 AD male and 2 AD female mice.

Immunohistochemistry confirmed Aβ accumulation in the brain (Figure 9). In order to provide a more quantitative measure of water-soluble and plaque-associated Aβ, sequential extraction of the brain was performed to extract water-soluble, Triton-soluble, and guanidinium hydrochloride-soluble Aβ, and levels of Aβ 40 and 42 were quantified via ELISA. At 8 months of age, no significant difference in total Aβ40, Aβ42, or Aβ42/Aβ40 ratio was observed. At 14 months of age, total Aβ40 ($p = .004$) and Aβ42 ($p = .018$) levels were significantly higher in AD males compared to AD females. Aβ42/Aβ40 ratio was significantly higher in AD females compared to AD males at 14 months of age ($p = .01$), but not at 8 months of age. The quantitative Aβ measures are shown in Table 2.

Total Aβ40 level showed a significant negative correlation with WB |G*| ($p = .03$, $r = -.71$), WB G_d ($p = .04$, $r = -.69$), WB G_l ($p = .02$, $r = -.73$), hippocampal |G*| ($p = .01$, $r = -.77$), hippocampal G_d ($p = .02$, $r = -.76$), and hippocampal G_l ($p = .01$, $r = -.78$) among all AD mice. Total Aβ42 level was significantly correlated with hippocampal |G*| ($p = .046$, $r = -.68$) and hippocampal G_l ($p = .039$, $r = -.69$), but not with hippocampal G_d or any WB MRE parameters among all AD mice. Neither Aβ40 nor Aβ42 was associated with the measured WB and hippocampal MRE parameters when AD males and females were investigated separately.

Figure 10 shows the relationship between the measured WB amyloid levels (ie, Aβ40, Aβ42, Aβ40/42 ratio) and the measured WB MRE parameters (ie, |G*|, G_d, G_l) in 14-month-old AD males (in blue color) and AD females (in orange color). These plots show a clear distinction between AD males and AD females with significantly higher amyloid levels in AD males, and significantly higher MRE parameters in AD females.

DISCUSSION

The most salient observations of our study are the following: (1) contrary to our hypothesis, there was no significant difference in viscoelastic properties of the brain between AD and WT mice at 11 or 14 months of age that corresponds to middle age (40-50 years) in humans. (2) When sex was not considered a variable, compared to WT mice, Aβ accumulation in the AD mice did not show significant effects on brain parenchymal viscoelasticity. However, Aβ accumulation may have sex-specific effects. (3) Over a period of 3 months, between the ages of 11 and 14 months, WB parenchyma showed age-related decreases in all viscoelastic parameters, while the hippocampi demonstrated the opposite. (4) The effect size of aging-related changes in viscoelastic properties of the brain were higher than any AD or sex-related effects.

To model AD, we used transgenic J20 mice, in which Aβ plaques appear first in the hippocampus at 1 month of age and Aβ deposition is progressive with diffuse plaques in the dentate gyrus and neocortex by 5-7 months and in the WB by 8-10 months.[19–21] Our biochemical and immunohistochemical analyses confirmed the accumulation of Aβ in the brain of each transgenic mouse. A study by Murphy et al. using the APP-PS1 AD mouse model ($n = 5$) found disease-specific softening

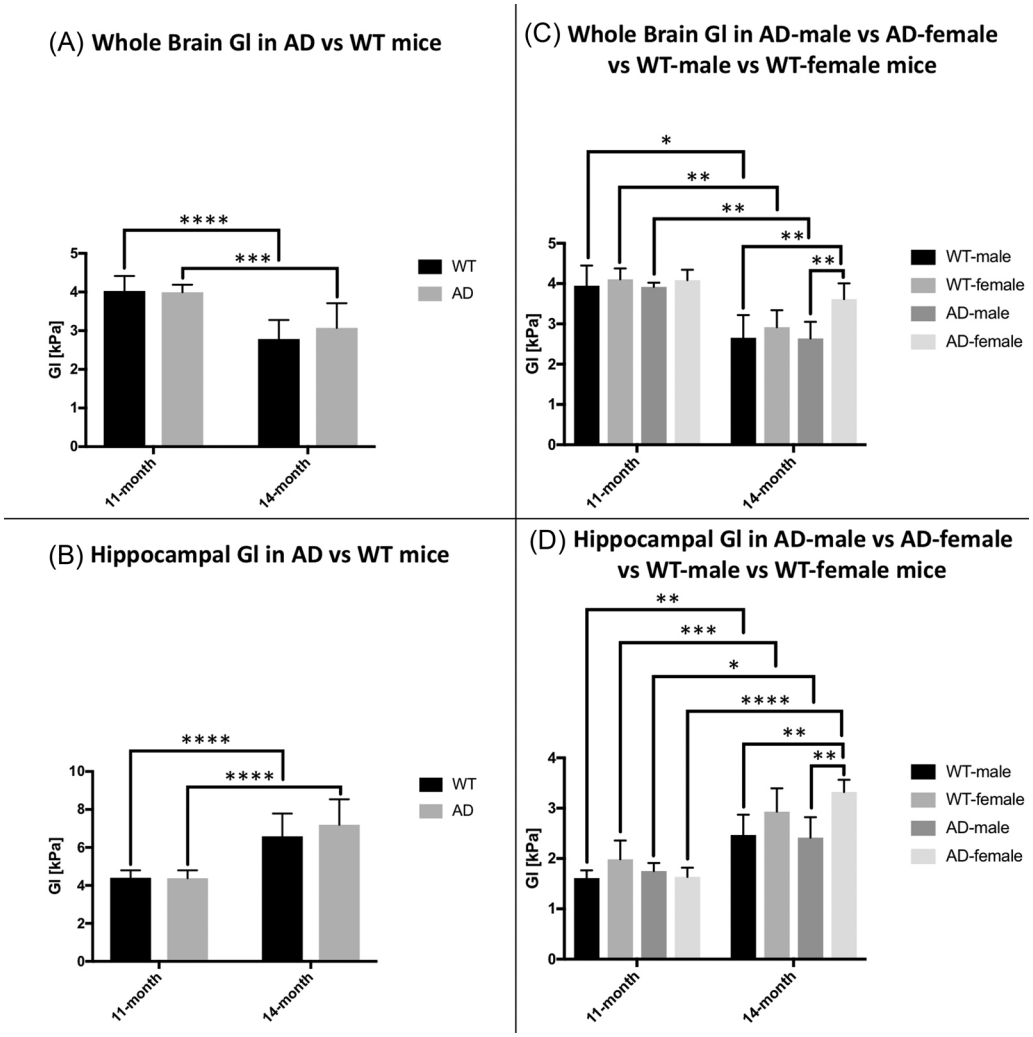

FIGURE 5 Cross-sectional and longitudinal comparisons of viscosity (G_I) in transgenic J20 versus wild-type mice at 11 and 14 months of age in the whole brain (A) and in the hippocampus (B). Cross-sectional and longitudinal comparisons of G_I in the four subgroups according to genotype and sex at 11 and 14 months of age in the whole brain (C) and in the hippocampus (D). Asterisks indicate the level of significance as follows: $^{*}p < .05$, $^{**}p < .01$, $^{***}p < .001$, $^{****}p < .0001$. AD, transgenic J20; WT, wild-type

in the WB parenchyma at a later disease stage (20 months) compared to WT mice ($n = 8$).[15] APP-PS1 mice, similar to our J20 mice, show widespread Aβ plaque deposition with neuronal and synaptic loss and microglia activation, but without mature neurofibrillary tangles.[29,30] AD-related WB softening has also been observed in several human MRE studies.[9–12,31] Our study found no AD-specific WB softening at either 11 or 14 months of age. It is conceivable that global softening of the brain parenchyma may manifest at a later disease stage in J20 mice. We attribute the observed changes in brain stiffness to normal aging processes, which demonstrated a differential and region-specific effect on brain stiffness: aging was associated with (1) a general decrease in viscoelasticity of the brain and (2) a general increase in viscoelasticity of the hippocampi. Our findings on aging are in line with previous studies on healthy humans, which have associated aging with softening of the brain parenchyma.[32,33] One of these studies also suggested that aging has a region-specific effect on subcortical stiffness,[33] finding significant softening in the striatum, thalamus, and amygdala in healthy older versus young adults, although they did not find a change in hippocampal stiffness.

Although genotype-based comparisons suggested no specific difference between AD and WT animals, analyses of genotype and sex combined revealed the following differences between males and females. (1) At 14 months of age, AD females showed higher WB and hippocampal viscosity and higher WB elasticity compared to AD and WT males. Differences between AD and WT females were not statistically significant but trended in the same direction. (2) WB elasticity and viscosity showed no significant change in AD females between 11 and 14 months of age, while there was a significant decrease in WB elasticity and viscosity in AD and WT males as well as in WT females over time. (3) The magnitude of increase in hippocampal viscosity over time was significantly larger in AD females versus WT males, but not compared to AD males or WT females. (The other hippocampal and WB MRE parameters did not show considerable difference between the four groups [ie, AD females, AD males, WT

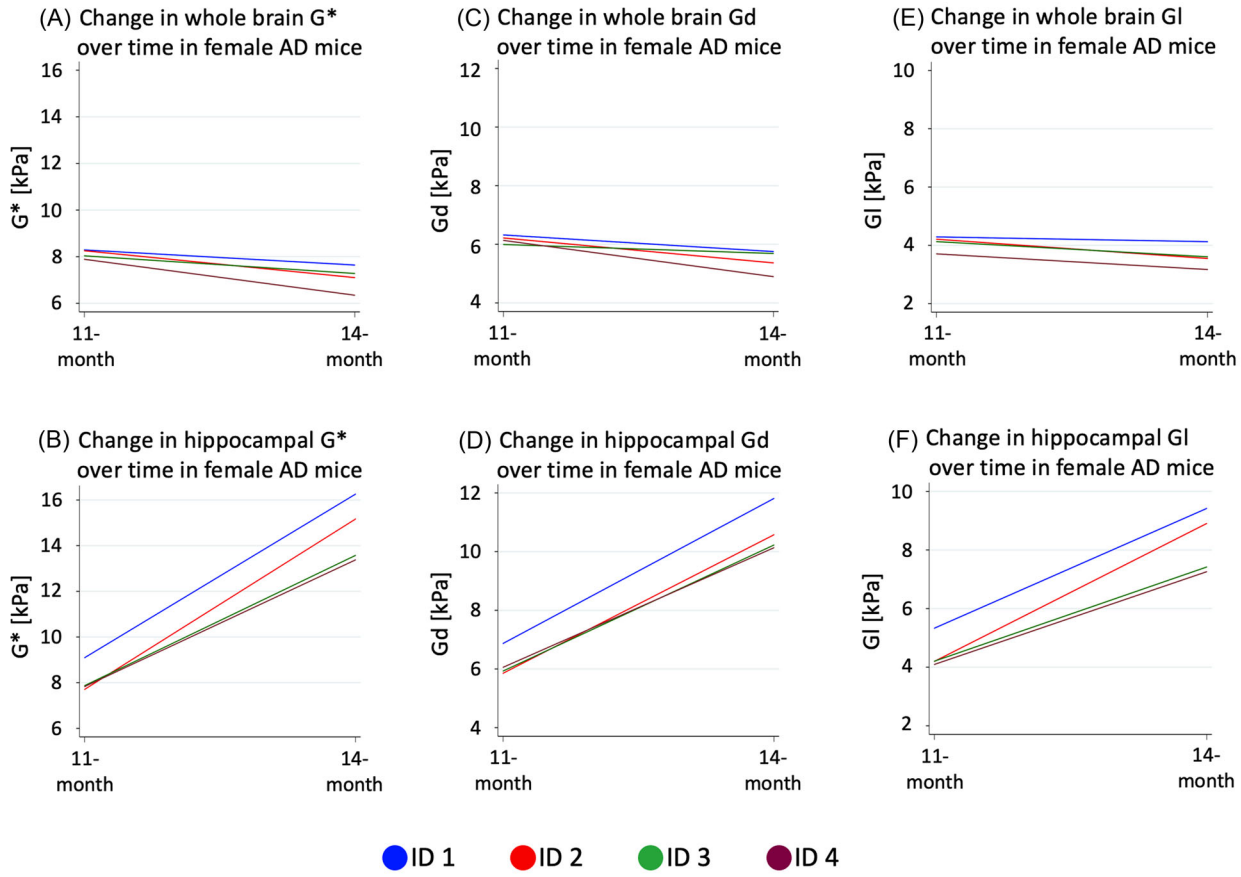

FIGURE 6 Changes in whole brain and hippocampal viscoelasticity (A and B), elasticity (C and D), and viscosity (E and F) in female transgenic J20 mice between 11 and 14 months of age. AD, transgenic J20; |G*|, viscoelasticity; G_d, elasticity; G_l, viscosity

TABLE 1 Evaluation of the whole brain and hippocampal Magnetic Resonance Elastography parameters in 11- and 14-month-old transgenic J20 and wild-type mice

		11 months of age						14 months of age					
		|G*| [kPa]		G_l [kPa]		G_d [kPa]		|G*| [kPa]		G_l [kPa]		G_d [kPa]	
		Mean	SD	Mean	SD	Mean	SD	Mean	SD	Mean	SD	Mean	SD
WT	Whole brain	7.88	0.70	4.03	0.39	5.83	0.56	5.60	1.02	2.79	0.49	4.26	0.85
(male + female)	Hippocampus	8.02	0.65	4.40	0.39	5.92	0.53	2.24	2.24	6.59	1.20	9.33	1.81
AD	Whole brain	7.92	0.26	3.99	0.20	6.00	0.21	6.12	1.14	3.07	0.64	4.69	0.86
(male + female)	Hippocampus	7.90	0.52	4.38	0.41	5.93	0.41	13.06	1.97	7.19	1.34	9.67	1.31
WT male	Whole brain	7.58	0.87	3.95	0.50	5.63	0.72	5.48	1.25	2.65	0.56	4.24	1.05
	Hippocampus	7.80	0.82	4.44	0.50	5.70	0.66	11.50	2.41	6.06	1.26	8.76	2.03
WT female	Whole brain	8.17	0.39	4.11	0.27	6.03	0.30	5.72	0.87	2.92	0.42	4.27	0.72
	Hippocampus	8.24	0.39	4.36	0.30	6.13	0.26	13.28	1.89	7.11	0.98	9.91	1.56
AD male	Whole brain	7.76	0.19	3.92	0.11	5.87	0.16	5.34	0.81	2.64	0.41	4.10	0.64
	Hippocampus	7.72	0.37	4.32	0.28	5.73	0.24	11.83	1.44	6.35	0.85	8.86	1.06
AD female	Whole brain	8.12	0.19	4.09	0.26	6.17	0.14	7.09	0.55	3.61	0.39	5.42	0.39
	Hippocampus	8.12	0.65	4.46	0.58	6.18	0.47	14.60	1.37	8.25	1.07	10.69	0.77

Note: Values in the table are presented as mean and standard deviation.

Abbreviations: AD, transgenic J20; |G*|, viscoelastic modulus; G_l, loss modulus (viscosity); G_d, storage modulus (elasticity); SD, standard deviation; WT, wild-type.

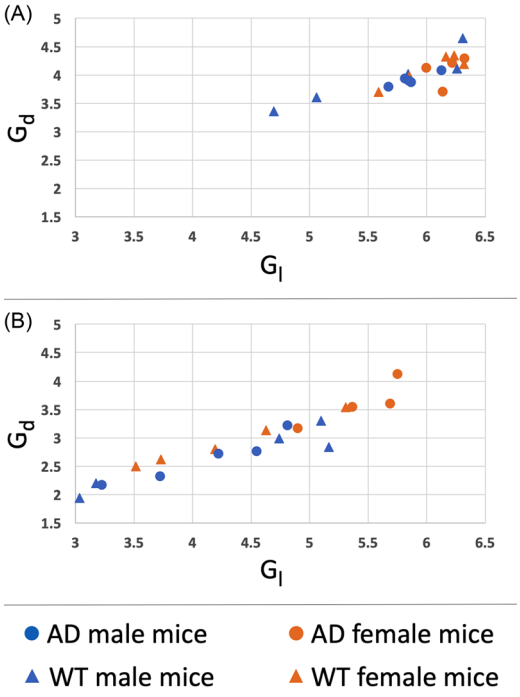

FIGURE 7 Whole brain elasticity versus whole brain viscosity in 11-month-old (A) and 14-month-old (B) wild-type male (blue triangle) and wild-type females (orange triangle), as well as transgenic J20 male (blue circle) and J20 female (orange circle) mice. AD, transgenic J20; G_d, elasticity; G_I, viscosity; WT, wild-type

females, WT males]). These results suggest a sex-specific effect might be at play in the aging process, with females developing a more pronounced hippocampal stiffening over time, compared to WT and AD males. This is in line with the human MRE study of McIlvain et al., which showed higher stiffness in the hippocampus (and in the amygdala) in female versus male adolescents.[32] In that study, the differences were not statistically significant, but the effect sizes were in the medium range.[32]

At an earlier disease stage (6 months) in the transgenic APP23 AD mouse model, Munder et al. found lower hippocampal viscosity in AD females ($n = 45$) versus WT females ($n = 39$).[14] Majumdar et al. also showed decreased WB viscoelasticity at 6 months of age and decreased hippocampal viscoelasticity at 4 months of age in 5XFAD females ($n = 9$) versus WT females ($n = 9$).[16] AD males were not investigated in the abovementioned studies.[14,16] APP23[34] and 5XFAD[35] mice are similar to J20 mice, in that they also show widespread Aβ plaque deposition with neuronal and synaptic loss and microglia activation, but without mature neurofibrillary tangles. A human MRE study has also associated AD with hippocampal softening,[11] while another human MRE study found no difference in hippocampal stiffness between AD patients and healthy controls.[31] Of note, both human MRE studies associated AD with WB softening.[11,31] In addition to in vivo studies, a recently published MRE phantom study also investigated the biomechanical effects of Aβ aggregates, and found that Aβ aggregates have significantly higher Y value compared to nonaggregated bovine serum albumin.[36] Compared to the study of Munder et al.[14] and Majumdar et al.,[16] our study was underpowered due to low sample size. The difference between AD females and WT females was not significant in our study, but trended in the opposite direction at 14 months of age (ie, hippocampus was stiffer in AD females compared to WT mice). This result requires further scrutiny. Our study is not the first one to find a trend for regional brain stiffening at a certain stage of AD. A recently published human MRE study suggested that amyloid positive subjects with mild cognitive impairment (MCI) and relatively low disease severity may have higher frontoparietal (FP) stiffness compared to AD patients with clinically diagnosed dementia and age and sex-matched healthy controls (HC).[9] This study had a low sample size ($n_{HC} = 16$, $n_{MCI} = 8$, $n_{AD} = 8$). Of note, only 2 out of the 8 MCI subjects showed higher FP stiffness than any HC or AD subjects. Female versus

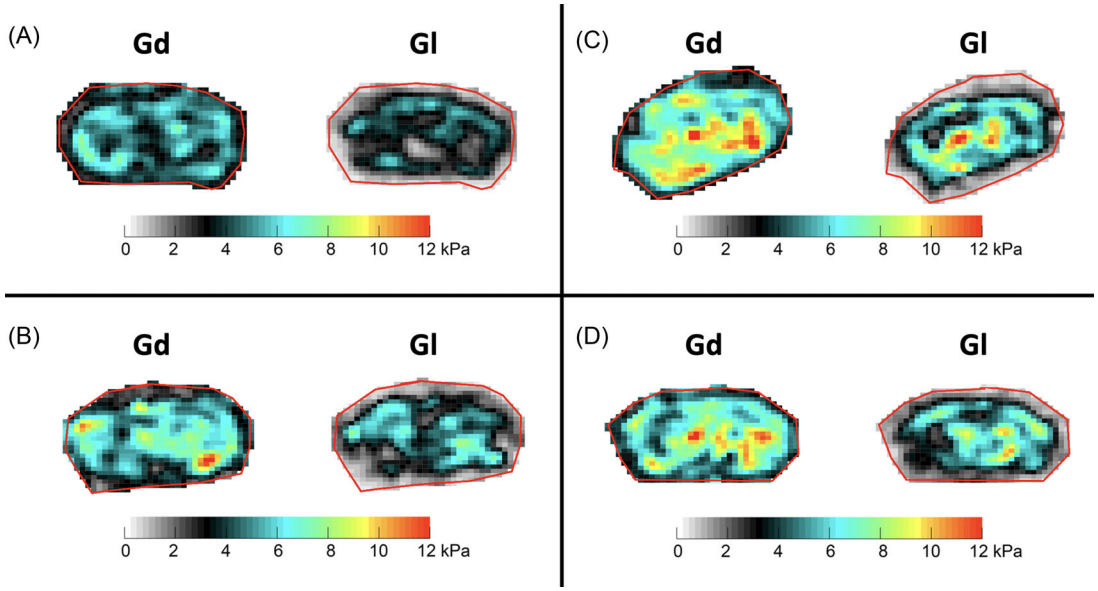

FIGURE 8 Elasticity and viscosity of two J20 male (A and B) and two J20 female mice (C and D). G_d, elasticity; G_I, viscosity

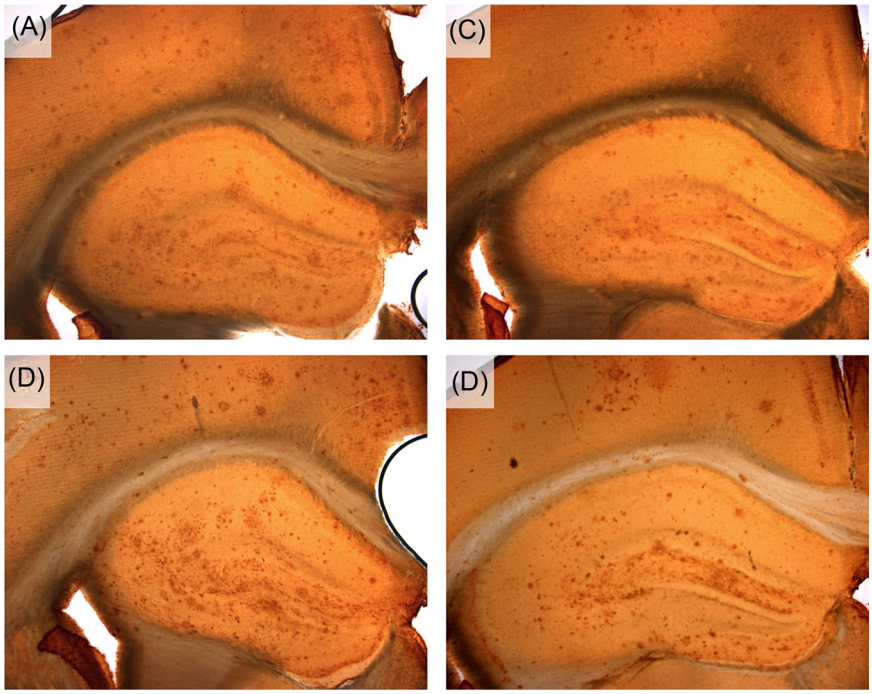

FIGURE 9 Representative microscope images of brain sections showing amyloid β accumulation in the hippocampus and cortex of two transgenic J20 mice with the highest (A and B) and the lowest (C and D) aggregated amyloid β levels. Immunohistochemistry was performed using a monoclonal antibody that recognizes the extreme N-termini of amyloid β (3D6). Dilution of 3D6 was 1:500 on panels A and C, and 1:1000 on panels B and D

TABLE 2 Brain parenchymal amyloid beta-40 (Aβ40) and -42 (Aβ42) levels in J20 mice at 8 and 14 months of age

	8 months of age					14 months of age				
	Aβ40		Aβ42			Aβ40		Aβ42		
	Mean	SD	Mean	SD	Aβ42:Aβ40 ratio	Mean	SD	Mean	SD	Aβ42:Aβ40 ratio
AD males + females ($n = 9$)	63.9	39.2	178.9	89.8	2.8	404.4	161.1	580.9	28.6	1.7
AD males ($n = 5$)	79.5	48.5	213.6	110.7	2.7	518.7	98.4	599.2	14.6	1.2
AD females ($n = 4$)	48.3	22.4	144.1	53.5	3.0	261.4	85.4	558.1	25.4	2.3

Note: Aβ40 and Aβ42 levels are expressed in nanograms of the amyloid compound per gram of brain tissue, that is, parts per billion.
Abbreviations: AD, transgenic J20; *n*, number of mice; SD, standard deviation.

male comparisons were not performed in this study. Future prospective cohort studies are required to investigate longitudinal changes and patterns in WB and regional viscoelasticity in AD using larger sample size and longitudinal MRE assessments from early to late disease stages.

There was twice as much Aβ40 in AD males versus AD females.[37] Levels of the more malignant amyloid, Aβ42, were slightly higher (7%) in AD males versus AD females. A previous immunoblot study also suggested that J20 males may have higher brain amyloid levels compared to J20 females, but this study did not perform quantitative amyloid assessments.[37] A previous human positron emission tomography (PET) study showed a negative association between cortical amyloid accumulation and brain stiffness in patients with AD.[9] In line with this study, we found strong negative correlations between brain parenchymal Aβ40 level and all MRE parameters at 14 months of age in mice. In fact, when WB amyloid levels (ie, Aβ40, Aβ42, Aβ40/42 ratio) were plotted against WB MRE parameters (ie, $|G^*|$, G_d, G_l), there was a clear distinction between 14-month-old AD males and AD females, with significantly higher amyloid levels in AD males, and significantly higher MRE parameters in AD females (Figure 10). The fact that there was no difference in viscoelastic properties between AD and WT males implies that the accumulation of Aβ plaques in males does not influence the shear modulus, at least to the level of plaque accumulation that was measured. This statement also holds true for females at the initial timepoint of 11 months. At the 14-month timepoint, however, significant differences were observed between AD females and both WT and AD males but not with WT females. Similar trending differences as observed with the males were observed with WT females. Of note, both G_d and G_l were higher in 75% AD females compared to AD and WT males and WT females at the 14-month timepoint (Figure 10). These observations suggest that viscoelastic properties are more susceptible to being influenced by Aβ in females.

Other pathologic mechanisms (eg, neuronal loss, synaptic loss, and gliosis[38]) may also affect brain stiffness in J20 mice. These mechanisms, in addition to the abovementioned aging-related effects, are likely more important in determining viscoelastic properties of the

JOURNAL OF NEUROIMAGING
THE OFFICIAL JOURNAL OF THE AMERICAN SOCIETY OF NEUROIMAGING

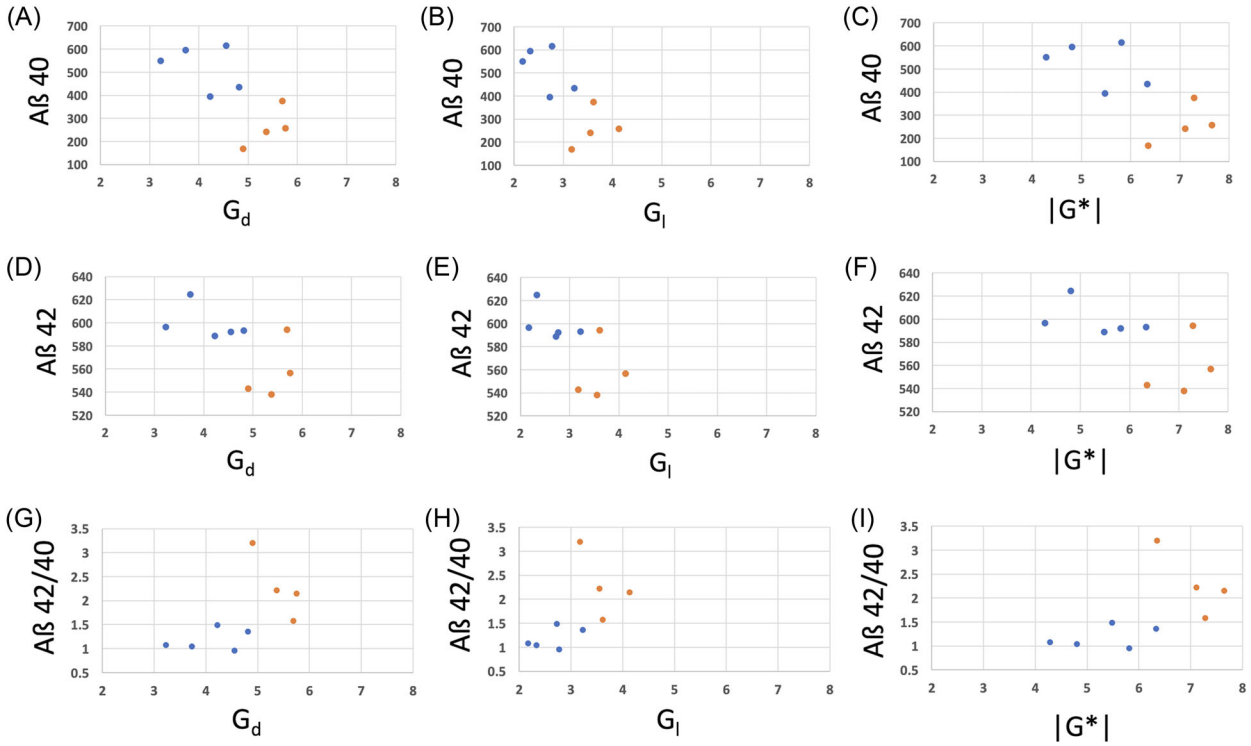

FIGURE 10 Relationship between the amyloid β data and Magnetic Resonance Elastography parameters at the 14-month timepoint. Amyloid β40 (A-C), β42 (D-F), and β40/42 ratio (G-I) as a function of elasticity (A, D, G), viscosity (B, E, H), and the magnitude of the viscoelastic modulus (C, F, I) in J20 male (blue circle) and J20 female (orange circle) mice. AD, transgenic J20; |G*|, magnitude of the viscoelastic modulus; G_d, elasticity; G_l, viscosity

brain than Aβ accumulation. Further studies are needed to investigate the direct effects of the aforementioned pathologic mechanisms on brain viscoelasticity.

Our study has the following limitations. (1) Some of our analyses (including the assessment of the association of viscoelasticity with Aβ40 and Aβ42 levels) might have been underpowered due to low sample size. (2) One of our AD female mice (Figure 6: ID 3) was ~1 month younger than the other AD and WT mice. However, none of the measured MRE parameters of this AD female mouse were the highest or lowest within the AD female subgroup. Therefore, we did not correct for age in our statistical analyses. (3) Correction for post hoc comparisons was applied within each ANOVA, but no additional correction was made for the total number of statistical analyses. (4) Viscosity and elasticity were investigated only in the WB parenchyma and hippocampus, but not in other brain regions. Since the WB and hippocampal MRE parameters changed in opposite directions over time, one could presume that WB viscosity and elasticity levels would show a more prominent decrease if hippocampi were excluded from the WB segmentation map. However, this analysis was not performed on our dataset.

To conclude, (1) we observed a difference between AD females and all other groups at 14 months of age that corresponds to 50 years of age in humans. (2) Amyloid plaque deposition may have sex-specific effects on viscoelastic properties, which require further scrutiny. (3) Aging had specific effects on viscoelasticity, namely, WB softening and hippocampal stiffening. Our study is of relevance for future studies investigating the diagnostic value of MRE in AD and other age-related processes.

ACKNOWLEDGMENT AND DISCLOSURE

M.P. has received personal compensation for consulting for ITineris Kft. K.S., N.N., J.P.M., W.M.T., R.S., T.L.Y. and S.P. report no disclosures. C.R.G has received research funding from Sanofi, the National Multiple Sclerosis Society, and the International Progressive Multiple Sclerosis Alliance, the U.S. Office for Naval Research, as well as travel support from Roche Pharmaceuticals; C.R.G owns stock in Roche, Novartis, GSK, Alnylam, Protalix Biotherapeutics, Arrowhead Pharmaceuticals, Cocrystal Pharma, and Sangamo Therapeutics.

ORCID

Miklos Palotai https://orcid.org/0000-0003-0268-6977

REFERENCES

1. Bisht K, Sharma K, Tremblay ME. Chronic stress as a risk factor for Alzheimer's disease: roles of microglia-mediated synaptic remodeling, inflammation, and oxidative stress. Neurobiol Stress 2018; 9:9-21.
2. Hardy J, Selkoe DJ. The amyloid hypothesis of Alzheimer's disease: progress and problems on the road to therapeutics. Science 2002;297:353-6.

3. American Psychiatric Association. Diagnostic and statistical manual of mental disorders. Washington, DC: APA; 2013.
4. Thal DR, Attems J, Ewers M. Spreading of amyloid, tau, and microvascular pathology in Alzheimer's disease: findings from neuropathological and neuroimaging studies. J Alzheimers Dis 2014;42(Suppl 4):S421-9.
5. Muthupillai R, Ehman RL. Magnetic resonance elastography. Nat Med 1996;2:601-3.
6. Sinkus R, Tanter M, Xydeas T, et al. Viscoelastic shear properties of in vivo breast lesions measured by MR elastography. Magn Reson Imaging 2005;23:159-65.
7. Mariappan YK, Glaser KJ, Ehman RL. Magnetic resonance elastography: a review. Clin Anat 2010;23:497-511.
8. Litwiller DV, Mariappan YK, Ehman RL. Magnetic resonance elastography. Curr Med Imaging Rev 2012;8:46-55.
9. Murphy MC, Jones DT, Jack CR Jr, et al. Regional brain stiffness changes across the Alzheimer's disease spectrum. Neuroimage Clin 2016;10:283-90.
10. Murphy MC, Huston J 3rd, Jack CR Jr, et al. Decreased brain stiffness in Alzheimer's disease determined by magnetic resonance elastography. J Magn Reson Imaging 2011;34:494-8.
11. Gerischer LM, Fehlner A, Kobe T, et al. Combining viscoelasticity, diffusivity and volume of the hippocampus for the diagnosis of Alzheimer's disease based on magnetic resonance imaging. Neuroimage Clin 2018;18:485-93.
12. ElSheikh M, Arani A, Perry A, et al. MR Elastography demonstrates unique regional brain stiffness patterns in dementias. AJR Am J Roentgenol 2017;209:403-8.
13. Murphy MC, Huston J 3rd, Ehman RL. MR elastography of the brain and its application in neurological diseases. Neuroimage 2019;187:176-83
14. Munder T, Pfeffer A, Schreyer S, et al. MR elastography detection of early viscoelastic response of the murine hippocampus to amyloid beta accumulation and neuronal cell loss due to Alzheimer's disease. J Magn Reson Imaging 2018;47:105-14
15. Murphy MC, Curran GL, Glaser KJ, et al. Magnetic resonance elastography of the brain in a mouse model of Alzheimer's disease: initial results. Magn Reson Imaging 2012;30:535-9.
16. Majumdar S, Klatt D. Longitudinal study of sub-regional cerebral viscoelastic properties of 5XFAD Alzheimer's disease mice using multifrequency MR elastography. Magn Reson Med 2021;86:405-14.
17. Fox J. The mouse in biomedical research. Amsterdam, The Netherlands: Elsevier; 2007.
18. Kilkenny C, Browne WJ, Cuthill IC, et al. Improving bioscience research reporting: the ARRIVE guidelines for reporting animal research. J Pharmacol Pharmacother 2010;1:94-9.
19. Mucke L, Masliah E, Yu GQ, et al. High-level neuronal expression of abeta 1–42 in wild-type human amyloid protein precursor transgenic mice: synaptotoxicity without plaque formation. J Neurosci 2000;20:4050-8.
20. Hong S, Beja-Glasser VF, Nfonoyim BM, et al. Complement and microglia mediate early synapse loss in Alzheimer mouse models. Science 2016;352:712-6.
21. Alzforum. J20 Phenotype Characterization. Available from: https://www.alzforum.org/research-models/j20-pdgf-appswind. Accessed 1 Mar 2022.
22. Schregel K, Nowicki MO, Palotai M, et al. Magnetic resonance elastography reveals effects of anti-angiogenic glioblastoma treatment on tumor stiffness and captures progression in an orthotopic mouse model. Cancer Imaging 2020;20:35.
23. Garteiser P, Sahebjavaher RS, Ter Beek LC, et al. Rapid acquisition of multifrequency, multislice and multidirectional MR elastography data with a fractionally encoded gradient echo sequence. NMR Biomed 2013;26:1326-35.
24. Franklin KBJ, Paxinos G. Mouse brain in stereotaxic coordinates. London: Academic Press; 2008.
25. Green MA, Bilston LE, Sinkus R. In vivo brain viscoelastic properties measured by magnetic resonance elastography. NMR Biomed 2008;21:755-64.
26. Fandos N, Perez-Grijalba V, Pesini P, et al. Plasma amyloid beta 42/40 ratios as biomarkers for amyloid beta cerebral deposition in cognitively normal individuals. Alzheimers Dement 2017;8:179-87.
27. Lehmann S, Delaby C, Boursier G, et al. Relevance of Abeta42/40 ratio for detection of Alzheimer disease pathology in clinical routine: the PLMR scale. Front Aging Neurosci 2018;10:138.
28. Singh SK, Srivastav S, Yadav AK, et al. Overview of Alzheimer's disease and some therapeutic approaches targeting abeta by using several synthetic and herbal compounds. Oxid Med Cell Longev 2016;2016:7361613.
29. Holcomb L, Gordon MN, McGowan E, et al. Accelerated Alzheimer-type phenotype in transgenic mice carrying both mutant amyloid precursor protein and presenilin 1 transgenes. Nat Med 1998;4:97-100.
30. Wengenack TM, Whelan S, Curran GL, et al. Quantitative histological analysis of amyloid deposition in Alzheimer's double transgenic mouse brain. Neuroscience 2000;101:939-44.
31. Hiscox LV, Johnson CL, McGarry MDJ, et al. Mechanical property alterations across the cerebral cortex due to Alzheimer's disease. Brain Commun 2020;2:fcz049.
32. McIlvain G, Schwarb H, Cohen NJ, et al. Mechanical properties of the in vivo adolescent human brain. Dev Cogn Neurosci 2018;34:27-33.
33. Hiscox LV, Johnson CL, McGarry MDJ, et al. High-resolution magnetic resonance elastography reveals differences in subcortical gray matter viscoelasticity between young and healthy older adults. Neurobiol Aging 2018;65:158-67.
34. Sturchler-Pierrat C, Staufenbiel M. Pathogenic mechanisms of Alzheimer's disease analyzed in the APP23 transgenic mouse model. Ann N Y Acad Sci 2000;920:134-9.
35. Oakley H, Cole SL, Logan S, et al. Intraneuronal beta-amyloid aggregates, neurodegeneration, and neuron loss in transgenic mice with five familial Alzheimer's disease mutations: potential factors in amyloid plaque formation. J Neurosci 2006;26:10129-40.
36. Bigot M, Chauveau F, Amaz C, et al. The apparent mechanical effect of isolated amyloid-beta and alpha-synuclein aggregates revealed by multi-frequency MRE. NMR Biomed 2020;33:e4174.
37. Quartey MO, Nyarko JNK, Pennington PR, et al. Age- and sex-dependent profiles of APP fragments and key secretases align with changes in despair-like behavior and cognition in young APPSwe/Ind mice. Biochem Biophys Res Commun 2019;511:454-9.
38. Wright AL, Zinn R, Hohensinn B, et al. Neuroinflammation and neuronal loss precede Abeta plaque deposition in the hAPP-J20 mouse model of Alzheimer's disease. PLoS One 2013;8:e59586.

How to cite this article: Palotai M, Schregel K, Nazari N, Merchant JP, Taylor WM, Guttmann CRG, et al. Magnetic resonance elastography to study the effect of amyloid plaque accumulation in a mouse model. J Neuroimaging. 2022;32:617–28. https://doi.org/10.1111/jon.12996